THE METHOD FOR HIGH ORDER MODES PARAMETERS ESTIMATION IN PERIODICAL STRUCTURES

V.V. Paramonov[1], D.V. Denisenko[1,2]
[1]Institute for Nuclear Research of the RAS, Moscow, Russia;
[2]Moscow Institute of Physics and Technology, Moscow, Russia
E-mail: paramono@inr.ru

The High Order Modes (HOM) parameters are calculated in traveling wave mode at one structure period for the reference set of the phase advance values, with real 3D geometry in the wide frequency range. For the structure with arbitrary length HOM parameters are interpolated basing on periodicity properties. The method resolution doesn't depends on the number of periods in the structure and allows reliably identify interesting and important HOM parameters for long structures and in high frequency region.

PACS: 41.60,41.75.L,41.75.H,84.40.A

INTRODUCTION

To estimate the multi-bunch effects due to long range wake fields induced in cavity-like obstacle, one has to know cavity response to the passing particle. The longitudinal $W^l(r_t,r_e,s)$ and the transversal $W^t(r_t,r_e,s)$ wake potentials for unit test and exiting point charges are expressed as [1,2]:

$$W^l(r_t,r_e,s) = 2\sum_m k_m^l \cos\left(\frac{w_m s}{c}\right) e^{-\frac{s}{ct_m}}, \qquad (1)$$

$$W^t(r_t,r_e,s) = 2r_t c\sum_m \frac{k_m^t}{w_m}\sin\left(\frac{w_m s}{c}\right) e^{-\frac{s}{ct_m}},$$

where r_t and r_e are radial positions for the test and the exiting charges, respectively, k^l_m and k^t_m are the loss factor and the kick factors for the m^{th} HOM in the cavity:

$$s = ct, \quad t_m = \frac{2Q_m}{w_m}, \qquad (2)$$

$$k_m^l = \frac{\left|\int_0^L E_{szm}(r=0)\,e^{\frac{iw_m z}{c}}dz\right|^2}{4U_m},$$

$$k_m^t = \frac{\left|\int_0^L E_{szm}(r=r_e)\,e^{\frac{iw_m z}{c}}dz\right|^2}{4r_e^2 U_m},$$

τ_m, Q_m, ω_m are the rise time, the quality factor and the frequency for the m^{th} mode, E_{szm} and U_m are the distribution for z component of electric field and stored field energy for the m^{th} mode. L is the cavity length.

To estimate the $W^l(r_t, r_e, s)$ and the $W^t(r_t, r_e, s)$ values we need in field distributions and RF parameters for all modes, which are possible in the cavity in a given frequency range. The length of the bunch is suppose much less as compared to the wavelength of the highest HOM. Suppose we have in the beam line enough long cavity, based on the periodical structure. In the cavity with N cells in the pass-band for each wave, there are, generally, N possible modes. Also there are a lot of pass-bands for different waves. For example, in the deflecting structure LOLA IV, [3], below frequency 4.5 f_0, where f_0 =2856 MHz is the operating frequency, there are ~ 250 pass-bands for different waves. The structure has N=104 cells and number of modes in the frequency range under consideration is of ~ 30,000. Even with powerful modern software for numerical simulations for fields distributions and mode frequencies, direct simulations for such modes amount are not realistic.

1. APPROXIMATIONS AND ASSUMPTIONS

For HOM parameters simulation we approximate the real structure by perfect periodical structure with the same number of cells, assuming also half cell termination, Fig.1. Such case we exclude from consideration input/output RF couplers, connection with beam pipe and another deviations from periodicity. This case we have to keep in mind possible influence of these elements on the results.

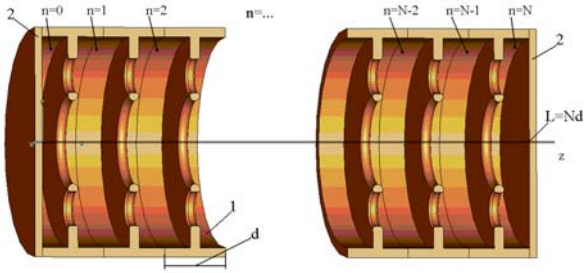

Fig.1. The cavity approximation as the finite length periodical structure

The structure period is assumed with mirror symmetry planes z=*const*. It allows us apply half cell structure terminations and decompose a standing wave fields in two traveling waves. The mirror symmetry planes x=0 or y=0 are not necessary. If such symmetry planes exist, it should be used to save time for numerical simulations.

2. PROCEDURE OF SIMULATIONS

To estimate HOM parameters in the cavity, based on the periodical structure in a wide frequency range, we simulate with modern software in the same frequency range parameters of traveling waves considering just one period of the structure for the reference set of the phase advance values θ_j, j=0,1,…J per period. The each component of a traveling wave field has real and imaginary parts:

$$E_{fj}(r,z) = \mathrm{B}E_j(r,z) - i\mathrm{Б}E_j(r,z),\ E_{bj}(r,z) = E^*_{fj}(r,z). \qquad (3)$$

For the structures with mirror symmetry in the period the real and the imaginary parts distributions along the axis have a conjugated parity. For definiteness we will assume distribution of the real part as the even function.

In Fig.2,a the cell of the deflecting structure for the PITZ Transverse Deflecting System [4] is shown together with the geometry for numerical simulations, Fig.2,b, and an example for real and imaginary E_z parts distributions, Fig.2,c.

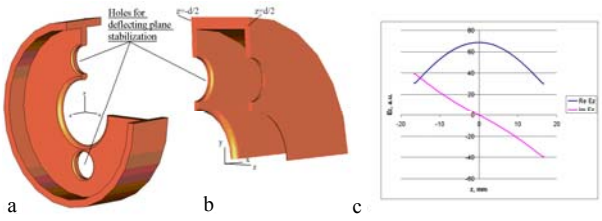

Fig.2. The cell of the deflecting structure(a), the geometry for numerical simulations (b) and an example for real and imaginary parts distributions (c) for the first monopole wave with θ=15°

If the fields distributions E_{fz} (3) of the traveling waves are known, for the structure with N periods a standing wave distribution E_{szm} for the m^{th} mode can be found as:

$$E_{szm}(z') = 2\mathrm{B}E_{fzm}(z)\cos(nq_m) + 2\mathrm{B}E_{fzm}(z)\sin(nq_m), \quad (4)$$

$$-\frac{d}{2}\mathrm{J}\ z\mathrm{J}\ \frac{d}{2},\ z' = z + nd,\ q_m = \frac{mp}{N},\ m,n = 0,1,\ldots N.$$

Substituting the expression (4) for longitudinal field of the m^{th} mode into (2), after transformation one can find for the loss factor k^l_m value:

$$k^l_m = \frac{\left\{I^{ee}_m\left[1+(-1)^m\cos(Nf_m)\right]+2S^{cc}_m I^{eo}_m(-1)^m\sin(Nf_m)-2I^{oo}_m S^{cs}_m\right\}^2}{4NU_0}+ \quad (5)$$

$$+\frac{\left\{I^{ee}_m\left[(-1)^m\sin(Nf_m)+2S^{cs}_m I^{eo}_m\right]\left[(-1)^m\cos(Nf_m)-1\right]+2I^{oo}_m S^{sc}_m\right\}^2}{4NU_0},$$

where

$$I^{ee}_m = \int_0^{d/2}\mathrm{B}E_{fzm}(z)\cos\left(\frac{f_m z}{d}\right)dz,\ I^{eo}_m = \int_0^{d/2}\mathrm{B}E_{fzm}(z)\sin\left(\frac{f_m z}{d}\right)dz, \quad (6)$$

$$I^{oo}_m = \int_0^{d/2}\mathrm{B}E_{fzm}(z)\sin\left(\frac{f_m z}{d}\right)dz,\ f_m = \frac{w_m}{c}d,$$

and

$$S^{cc}_m = \sum_{n=1}^{N-1}\cos(nq_m)\cos(nf_m),\ S^{sc}_m = \sum_{n=1}^{N-1}\sin(nq_m)\cos(nf_m), \quad (7)$$

$$S^{cs}_m = \sum_{n=1}^{N-1}\cos(nq_m)\sin(nf_m),\ S^{ss}_m = \sum_{n=1}^{N-1}\sin(nq_m)\sin(nf_m).$$

The huge formula (5) with (6) and (7) describes the general case, including both synchronous ($\theta_m = \phi_m$) and not synchronous interaction between the wave with and relativistic particle. In the case of synchronous interaction this formula is very simple:

$$k^l_{m\max} = \frac{N^2\left(I^{ee} + (-1)^{nb} I^{oo}\right)}{4U_0}, \quad (8)$$

where nb is the integer part of ratio $(2\pi f_m)/(\theta_o f_o)$, where θ_o and f_o are the operating phase advance and operating frequency of the structure, respectively.

The kick factor value for dipole-like modes can be estimated with the same way, calculating E_z in integrals of interactions (6) at some distance r_e, see (2).

Integrals of interaction (6) are calculated at the set of reference θ_j values and there are the smooth θ_m and ϕ_m functions. For intermediate θ_m values in the long structure interpolation is used.

3. MODEL VERIFICATION

To check the correctness of the proposed model and huge intermediate transformation to the final expression (5), we can directly simulate the field distributions in the relatively short N=16 or N=46 cells structures [4], for the first pass-bands of monopole modes TM_{01} and dipole modes HE_{11}, assuming standing wave regime, and calculate k^l_m and k^t_m values for each mode from (2). The models for these direct simulations are shown in Fig.3.

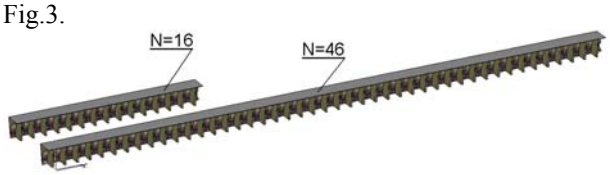

Fig.3. The models for direct fields distributions simulations in the first TM01 and HE11 pass-bands

The results of this comparison are plotted in Fig.4. The solid lines just connect points of k^l_m and k^t_m values for discrete θ_m values.

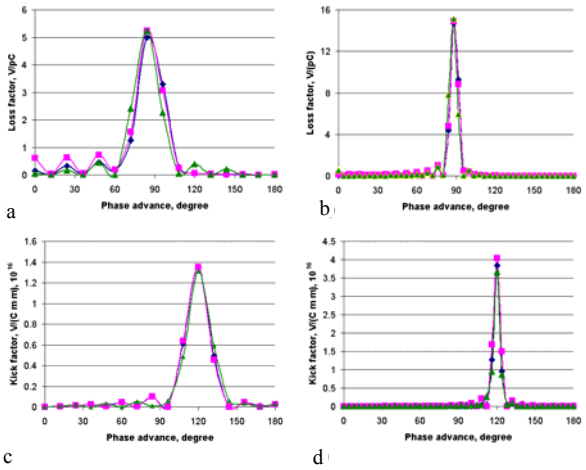

Fig.4 The k^l_m and k^t_m values calculated from direct field distributions simulations (blue) and from (5) (magenta) for N=16 cells (a,c) and N=46 (b,d). The green triangles are for the full end cell termination

One can see in Fig.4 a good coincidence of results, obtained with different approaches. For the most important the maximal k^l_m and k^t_m values the relative difference is inside of 5%. The huge formula (5) for k^l_m and k^t_m values in long periodical structures is correct and can be used for estimations.

As one can see from the Fig.4, k^l_m and k^t_m dependences on θ_m have a bell-like shape. The width of this bell is narrower for longer structure, but all time three modes belong to the peak.

4. INTERACTION OF PARTICLE WITH WAVE IN THE FINITE STRUCTURE

In the aperture of periodical structure the component E_z both for traveling E_f and for standing E_s waves can be expanded into series over space harmonics [5]:

$$E_{fj}(x,y,z) = \sum_p a_{jp}(x,y)e^{\frac{iq_p\cdot z}{d}},$$

$$E_{sjm}(x,y,z) = \sum_p 2a_{jp}(x,y)\cos\left(\frac{q_{mp}z}{d}\right), \quad (9)$$

$$q_{p,m} = q_{o,m} + 2pp,\quad p = 0,\pm 1,\ldots,\pm\Gamma.$$

For each space harmonic in (9) we can directly estimate the integral of interaction $S(\theta_{mp})$ with the relativistic particle, which is in the numerator for k^l_m and k^t_m values in (2).

ISSN 1562-6016. ВАНТ. 2012. №4(80)

$$S(Q_{mp}) = \int_0^{Nd} \cos\left(\frac{Q_{mp} z}{d}\right) e^{-i\frac{w_m z}{c}} = \tag{10}$$

$$= \frac{1}{2}\left(\frac{e^{-iNd\left(\frac{w_m}{c}+\frac{Q_{mp}}{d}\right)} - 1}{i\left(\frac{w_m}{c}+\frac{Q_{mp}}{d}\right)} + \frac{e^{-iNd\left(\frac{w_m}{c}-\frac{Q_{mp}}{d}\right)} - 1}{i\left(\frac{w_m}{c}-\frac{Q_{mp}}{d}\right)}\right).$$

The real, the imaginary parts and the amplitude of $S(\theta_{mp})$ for the first monopole pass-band TM_{01} in the deflecting structure [4] are plotted in Fig.5.

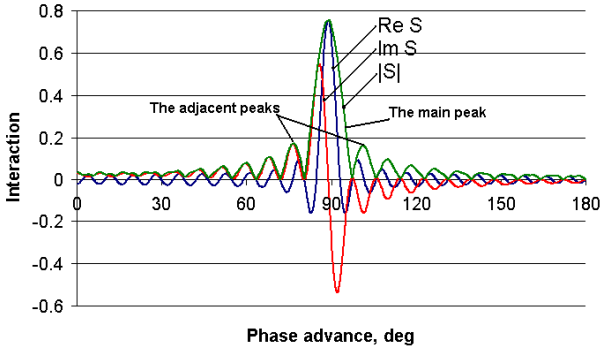

Fig.5. The plots of the real (blue), the imaginary (red) parts and the amplitude (green) for integral of interaction $S(\theta_{mp})$ for the first monopole pass band in the deflecting structure [4], N=46

One can see in Fig.5 for the $S(\theta_{mp})$ amplitude the same bell-like shape, as in Fig.4. As one can directly find from (10), the maximal value $|S(\theta_{mp})|_{max} = Nd/2$ and is realized for the synchronous case $\theta_{mp}/d = \omega_m/c$. The width of the main peak, see Fig.5, is of $d\theta = 4\pi/N$ and for longer structures this peak is narrowed. The modes separations in the structure is of π/N and all time at least three modes belong to the main peak.

The decreasing adjacent peaks, Fig.5, have the width of $d\theta = 2\pi/N$. The nearest peaks have the maximal value of $Nd/(3\pi)$. With respect the with to the main peak, the nearest adjacent peaks are $3\pi/2 \sim 4.5$ times lower. In the expressions (2) interaction $S(\theta_{mp})$ is in the second power and all modes, which do not belong to the $2\pi/N$ vicinity of the synchronous point, will have at least one order lower k^l_m and k^t_m values.

5. COMPARISON WITH THE RESULTS OF TIME DOMAIN SIMULATIONS

To check this method additionally, HOM parameters simulations were performed for the LOLA IV deflecting structure [3] in the frequency range $f < 4.5\ f_0$ and our results were compared with the results, obtained for the same structure with the time domain approach [6]. For comparison our simulations were performed for a reference structure, which is in 2D approximation, similar to one, shown in Fig.2, but without holes for deflection plane stabilization. For the monopole modes in the reference LOLA IV structure calculated dispersion diagram is shown in Fig.6. The main reason for such 2D approximation is only limitations for software, used in [6].

In Fig.6 all zones for all points of synchronous interactions for different branches of the dispersion diagram are marked with numbers. Numerical results of comparison are presented in the Table, where N_b is the brunch number in the dispersion diagram (see Fig.6).

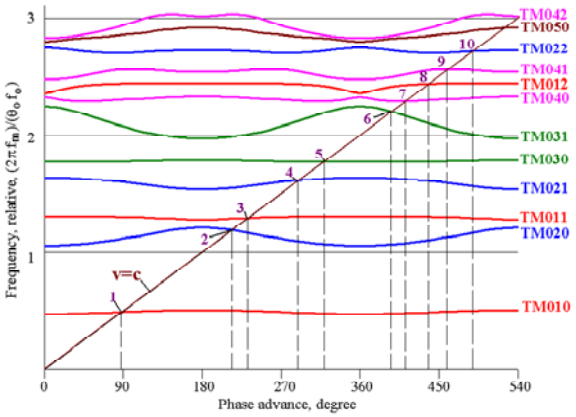

Fig.6. Dispersion diagram for monopole modes in the reference LOLA IV structure

The loss factor values for the monopole modes with $k^l_m > 1$ V/(pC) in the LOLA IV reference structure. Results from [6] are presented for comparison

N_b	f_m, GHz	k^l_m, V/pC	k^l_{mmax}, V/pC	Q_m	f_m,[6], GHz	k^l_m,[6] V/pC
1	2.088	1.35	34.87	13380		
1	2.092	1.35	33.29	13369		
1	2.094	29.45	32.49	13363	2.11	34.6
1	2.097	23.32	31.70	13357		
1	2.099	2.28	30.92	13352		
2	5.064	3.89	4.38	25467	5.09	3.26
2	5.071	2.73	4.65	25451		
3	5.557	4.66	5.25	13543		
3	5.555	4.20	5.52	13571	5.57	5.76
4	6.894	1.01	3.50	28290		
4	6.890	3.92	4.02	28113		
4	6.886	3.12	4.57	27936	6.93	4.7
5	7.582	3.86	6.25	17228		
5	7.582	6.14	6.44	17323	7.62	6.4
5	7.582	1.46	6.63	17418		
8	10.492	1.44	1.52	18173	10.5	1.3
9	10.930	1.92	3.16	24778	11	2.6
9	10.929	2.58	2.71	24784		
10	11.660	2.47	2.76	20733	11.7	2.8
10	11.662	1.99	2.62	20614		

For each pass in the time domain simulations just one mode is shown. It is not a fundamental limitation, but to show a fine modes structure for each zone of interactions time domain will is required fields simulations at much longer distances $s > c/(f_{m+1}-f_m) \sim 100\ m$, as it accepted usually $(s >> c/f_m \sim 1\ m)$. With such requirement the time domain simulation for long structures with short bunches becomes a huge computational problem. As one can see from Table, the frequency value for interacting modes coincides with reasonable precision. The single loss factor value k^l_m for each pass band coincides very well with our estimation for the maximal loss factor value k^l_{mmax} (8) for this pass band. But, our simulations show in the vicinity of synchronous point at each pass band at least two modes with k^l_m values, comparable with k^l_{mmax}.

As the result, over all loss factor value, summarized over all modes at the pass band, from our approach is more than two times larger, as from usual time domain simulations. For our approach such difference is motivated well both with the physical consideration in Section 5 and direct numerical verification in Section 4.

Similar comparison has been performed for kick factor values k^l_m for the same LOLA IV reference structure. The same coincidence in frequencies for synchronous points and kick factor values, and the same difference in the number of interacting modes at each pass band. Also the same is the conclusion for over all kick factor value for each pass band – our approach provides more than two times value, as compared to usual medium *s* range tine domain simulations.

5.1. MODE MIXING EFFECT ON LOSS AND KICK FACTORS VALUES

The total modes spectrum of the structure, especially in high frequency region, is rather complicated. But 2D approximation reference structure option we can clearly separate monopole and dipole modes, which are mostly dangerous for the multi bunch effects. And in reference structures all multi – pole modes have E_z=0 at the structure axis.

In the real 3D structure all modes have more complicated field distributions. If a 3D addition (with respect to 2D reference structure) is not so strong, one can treat fields in the 3D structure with mode mixing effect, considering 3D structure fields as composed from reference modes of 2D reference structure.

Loss and kick factor values were calculated in the real 3D LOLA IV geometry, taking into account holes for deflecting plane stabilization, see Fig.2, in the same frequency range $f < 4.5\ f_0$. The first pass bands both for monopole and dipole modes are well separated in frequency from another branches of dispersion diagram, resulting in k^l_m and k^t_m values with negligible difference between real 3D and approximated 2D structures. For higher pass bands with frequencies $f > 1.5\ f_0$ real mode mixing effect exists, resulting in more smooth loss factor redistribution between branches of the total dispersion diagram.

Basing on the theory of coupled modes, but omitting huge formulas and transformations for multi coupled modes analysis, and results of direct simulations for 3D real structures and 2D approximations, qualitative conclusion can be done. For not strong 3D deviations from 2D approximated structure geometry the mode mixing effect produce more smooth distribution for loss factor values k^l_m between branches of the total dispersion diagram for 3D structure. But the over all loss factor value in the wide frequency range is the same, both for real 3D and approximated 2D structures, with the precision in several percents.

For kick factor values such conclusion is not valid and large difference, than several percents, was detected between 3D and 2D approximations.

SUMMARY

The method for HOM parameters estimations in periodical structures is developed. HOM parameters are calculated in the wide frequency range at one structure period for the reference set of the phase advance values, with real 3D geometry. For the structure with arbitrary length HOM parameters are interpolated basing on periodicity properties, meaning the problem dimensionality decreasing for simulations. Wake fields excitation is treated as an interaction of particle with finite length periodical structure. It results in the detection of the fine structure for interacting modes in vicinities of each point of synchronous interaction at different modes pass bands. Detection of such fine modes structure with time domain approach for long structures with a short bunches will require enormous efforts in simulations.

The method was applied for HOM parameters estimation and study in the X-FEL TDS [4].

This work was supported by the Ministry of Education and Science of the Russian Federation, the contract № 16.518.11.7037

REFERENCES

1. K.L.F. Bane, P.B. Wilson, T. Weiland. *Wake fields and Wake Fields Acceleration.* SLAC-PUB-3528, SLAC, 1984.
2. T. Weiland, R. Wanzenberg. Wake fields and Impedances // *DESY M 91-06, DESY*, 1991.
3. O.H. Altenmueller, G.A. Loew. Design and Applications of RF Separator Structures at SLAC. SLAC-PUB-0135, 1965 // *Intern. Conf. on High Energy Part. Accel, Fraskatti, Rome*, 1965.
4. L. Kravchuk, et al. Layout of the PITZ Transverse Deflecting System for Longitudinal Phase Space and Slice Emmitance Measurements // *Proc. 2010 Linac Conference*, Tsukuba. 2011, p.416.
5. G.A. Loew, R.B. Neal. Accelerating structures // *In Linear Accelerators, ed. P. Lapostole, A. Septier*. Amsterdam: «North-Hol. Pub. Co». 1970, p.39-107.
6. I. Zagorodnov, T. Weiland. Wake Fields Generated by the LOLA IV Structure and 3rd Harmonic Section in TTF-II // *TESLA Report 2004-01*, DESY, 2004.

Статья поступила в редакцию 24.09.2011 г.

МЕТОД ВЫЧИСЛЕНИЯ ХАРАКТЕРИСТИК ВЫСШИХ МОД В ПЕРИОДИЧЕСКИХ СТРУКТУРАХ

В.В. Парамонов, Д.В. Денисенко

ВЧ-характеристики высших мод колебаний (ВМК) рассчитаны в режиме бегущей волны в широком диапазоне частот на одном периоде структуры в трехмерном приближении для опорного набора набегов фазы поля на период. Для структуры с произвольным числом периодов ВМК параметры интерполируются исходя из свойств периодичности. Разрешение метода не зависит от числа периодов в структуре и позволяет выявить важные особенности ВМК в длинных структурах и диапазоне высоких частот.

МЕТОД ОБЧИСЛЕННЯ ХАРАКТЕРИСТИК ВИЩИХ МОД У ПЕРІОДИЧНИХ СТРУКТУРАХ

В.В. Парамонов, Д.В. Денисенко

ВЧ-характеристики вищих мод коливань (ВМК) розраховані в режимі бігучої хвилі в широкому діапазоні частот на одному періоді структури в тривимірному наближенні для опорного набору набігів фази поля на період. Для структури з довільним числом періодів ВМК параметри інтерполіруються виходячи з властивостей періодичності. Дозвіл методу не залежить від числа періодів в структурі і дозволяє виявити важливі особливості ВМК у довгих структурах і діапазоні високих частот.